Halogenation dictates the architecture of amyloid peptide nanostructures

Article

Accepted Version

Halogenation Dictates Architecture of Amyloid Peptide Nanostructures

Andrea Pizzi,[1] Claudia Pigliacelli,[2] Alessandro Gori,[3] Nonappa,[2] Olli Ikkala,[2] Nicola Demitri,[4] Giancarlo Terraneo,[1] Valeria Castelletto,[5] Ian W. Hamley,[5] Francesca Baldelli Bombelli,[1] Pierangelo Metrangolo*[1,2,3]

[1] Laboratory of Supramolecular and BioNano Materials (SupraBioNanoLab), Department of Chemistry, Materials, and Chemical Engineering "Giulio Natta", Politecnico di Milano, Via Luigi Mancinelli 7, Milano I-20131, Italy

[2] Department of Applied Physics, Aalto University, Espoo, FI-02150, Finland

[3] ICRM-CNR, Laboratory of Peptide and Protein Chemistry, Via Mario Bianco 9, 20131 Milano, Italy

[4] Elettra – Sincrotrone Trieste, S.S. 14 Km 163.5 in Area Science Park, 34149 Basovizza – Trieste, Italy

[5] Department of Chemistry, University of Reading, Whiteknights, Reading, RG6 6AD, UK

Supporting Information Placeholder

ABSTRACT: Halogenation is reported as an approach to tune amyloidogenic peptide self-assembly. Seven halogenated derivatives of the pentapeptide KLVFF show supramolecular polymorphism, affording peptide nanoparticles, 'cotton balls', straight tapes, twisted or helical ribbons according to position, nature and number of the introduced halogen atoms. Our findings demonstrate that halogenation may represent a general strategy to modulate peptide self-assembly and design new amyloidal assemblies.

Alongside pathological roles in many diseases, *e.g.*, Alzheimer's, Parkinson's, Creutzfeldt-Jacob, and Huntington's,[1] amyloid peptide architectures have found many other nonbiological applications[2] as forming highly ordered nanomaterials.[3] Together with their biocompatibility and ease of production,[4] amyloidogenic peptides show a very versatile polymorphic behavior yielding a broad range of hierarchical structures, such as tapes, ribbons, fibers, nanoparticles, and nanotubes.[5,6] Subtle variations in the experimental conditions, peptide sequence or its chemical functionalization may impact the self-assembly pathway and, consequently, the resulting nanostructure.[7]

Despite representing a powerful tool to produce various nanoobjects, amyloid intrinsic polymorphism may, however, limit the controlled construction of specifically designed nanostructures. The possibility of tuning such polymorphic behavior is still in its early stages.[8,9] For example, amino acid sequence in constitutionally isomeric tetrapeptide amphiphiles has recently been shown to dictate nanostructural architecture.[10] Chemical functionalization of the peptide sequence has also been demonstrated to be a powerful tool for controlling amyloid self-assembly.[11,12] In this regard, polymer conjugation has extensively been studied as a particularly fruitful strategy.[13]

Recently, some of us demonstrated that halogenation at the *p*-position of one or both phenylalanine (Phe) benzene rings of the human calcitonin-derived fibrillogenic peptide sequence **DFNKF**,[14] promotes amyloid self-assembly. Hydrogel formation efficiency is also promoted by the rich variety of noncovalent interactions given by halogen atoms,[15] among these, the halogen bond.[16] In this context, here we applied this strategy to dictate the

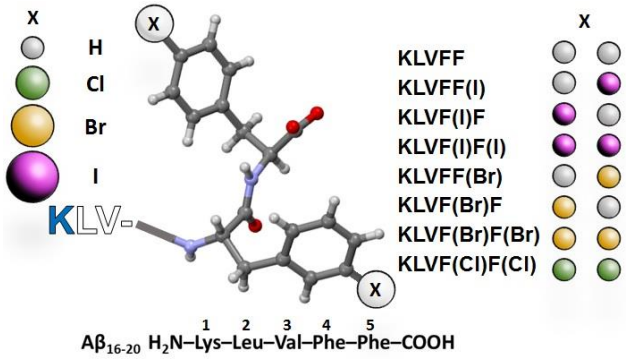

Figure 1. Chemical structures of halogenated **KLVFF** peptides.

architectures of the obtained amyloid nanostructures starting from the amyloid β (Aβ) peptide-derived core-sequence **KLVFF** (H_2N-Lys-Leu-Val-Phe-Phe-COOH) (Figure 1). Thanks to the presence of the –FF– motif, this pentapeptide has a highly pronounced aggregation propensity, as proved both computationally[17-19] and experimentally.[20]

By single-atom hydrogen-for-halogen replacement at the *p*-position of either one or both Phe benzene rings of **KLVFF**, we demonstrate here that halogenation dictates controlled formation of various nanostructures. Nanoparticles, ribbons, fibrils, and "cotton balls" are specifically obtained depending on the number, position, and nature of the introduced halogen atoms. This is remarkable for such a modest chemical structure modification. These results reveal the potential of controlling the morphology of amyloid nanostructures through single-point halogenation of amino acid sequence.

To study the effect of the introduction of halogen atoms at specific positions of the **KLVFF** pentapeptide on its self-

assembly, we obtained the 4-*p*-X-Phe derivative, the 5-*p*-X-Phe derivative, as well as the 4,5-bis-*p*-X-Phe derivative, where X = I, Br, Cl, H (Figure 1). Importantly, all of the studied peptides carry free amino (N) and carboxyl (C) termini.

Aqueous samples of the peptides were prepared by direct dispersion in milli-Q water (see Supporting Information, SI). As an indication of the formation of fibrils,[19] hydrogelation tests were run and minimum gelation concentrations (MGCs) determined. **KLVF(I)F**, **KLVF(Br)F**, and **KLVF(I)F(I)** were found to form gels (Figure 2) above MGCs that were much

Figure 2. 15 mM peptide water samples upon aging 48h at r.t.

lower than the wild-type fragment **KLVFF** (60 mM) (Table S1).[20] The best gelator of the series, **KLVF(I)F**, showed an MGC of 7 mM (0.5 % w/w, *i.e.*, 8-fold lower than **KLVFF**). This already indicates that halogenation has a clear effect on the peptide self-assembly process, promoting fibrillation, as previously observed.[14] A working concentration of 15 mM was chosen to compare all the gel-forming halogenated peptides in the same conditions (Table S2). The efficiency of gel formation in these conditions followed the order **KLVF(I)F** > **KLVF(Br)F** > **KLVF(I)F(I)**. The first two mono-halogenated peptides yielded homogeneous and transparent gels. The bis-iodinated one, instead, formed a homogeneously opaque, off-whitish ("milky"), gel.

Characterization of the different halogenated peptide hydrogels was done by oscillatory rheology (ring-cast method) using the 15 mM concentration samples. The mono-iodinated peptide was confirmed to form the stiffest gel, which is reflected in its higher elastic modulus (G'~ 10^3 Pa and G''~ 10^2 Pa after two weeks aging; Figure S1 in the SI). The trends of G' and G'' values parallel that of gel formation efficiency and MGCs, *i.e.*, **KLVF(I)F** > **KLVF(Br)F** > **KLVF(I)F(I)**. In particular, the latter yielded the weakest gel, which turned stiff enough for rheological measurement only after 2-week aging.

All other peptides, *i.e.*, **WT**, **KLVFF(I)**, **KLVFF(Br)**, **KLVF(Br)F(Br)** and **KLVF(Cl)F(Cl)** did not form gels in the same experimental set-up and all but **KLVF(Br)F(Br)** afforded colorless solutions. **KLVF(Br)F(Br)**, instead, formed a homogeneously opaque, "milky" solution.

Interestingly, the pairs **KLVF(I)F** – **KLVFF(I)** and **KLVF(Br)F** – **KLVFF(Br)** are constitutional isomers though show dramatically different macroscopic behavior (gels *vs.* solutions), highlighting the specific role of the position of the halogen atom in the peptide sequence. Furthermore, the different behavior of **KLVF(I)F(I)** compared to **KLVF(Br)F(Br)** also highlights a potential role of halogen atom polarizability in the self-assembly process. Hydrophobic interactions should not play a major role in determining the observed 15 mM-solution behaviors, *e.g.*, hydrogel formation,[21] because mono-halogenated peptides have similar hydrophobicity, and the bis-brominated derivative is more hydrophobic than the mono-halogenated ones (Table S3). Also, electrostatic interactions cannot fully explain differences between the studied peptides.

The "milky" solution given by the **KLVF(Br)F(Br)** peptide was analyzed by using Polarized Optical Microscopy (POM) at room temperature. Birifringent textures were observed after 48 hour from preparation (Figure S2), indicating that at a 15 mM concentration, **KLVF(Br)F(Br)** self-assembles into lyotropic liquid crystalline phases at r.t. In particular, the observed textures, *i.e.*, Maltese crosses, are characteristic of smectic A phases, which indicate a lamellar-type organization.

In order to investigate whether different solution behavior is related to a different morphology of the halogenated peptide assemblies, imaging was performed using Transmission Electron Microscopy (TEM; 15 mM, 48h after preparation) (Figure 3).

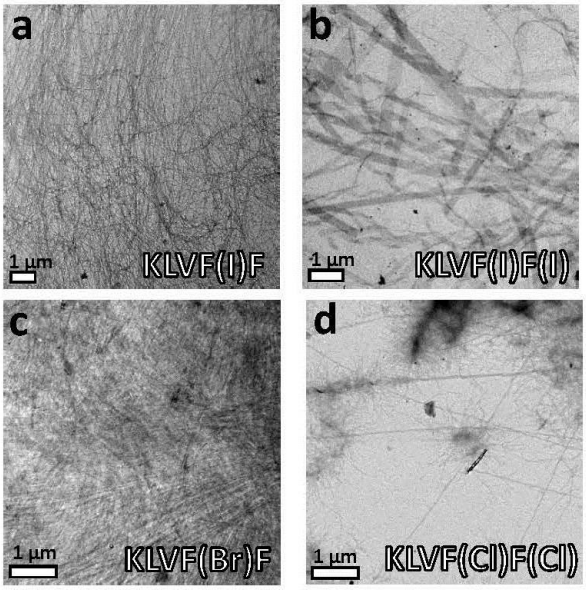

Figure 3. TEM images of 15 mM dried gels/solutions of the halogenated derivatives of **KLVFF** showing different architectures upon varying position, number, and nature of the halogen atoms.

As expected, the peptides forming the strongest gels – **KLVF(I)F** and **KLVF(Br)F** – showed a dense network of entangled fibrils (Figure 3a,c), which is rather usual for amyloidal hydrogels. The weakest gel-forming peptide **KLVF(I)F(I)**, instead, formed an entangled network of ribbon-like fibers, either straight or twisted, which may explain the "milky" appearance of the gel due to light scattering (Figure 3b). A few long, thin, and straight fibrils were also observed in the case of **KLVF(Cl)F(Cl)**, which, however, do not lead to the formation of the dense and entangled network needed for gel formation (Figure 3d).

The non- gel-forming peptides **KLVFF(I)** and **KLVF(Br)F(Br)** showed the most interesting morphologies. In particular, spherical nanoparticles (NPs) of around 50 nm were observed for the former (Figure 4a), while spherical structures (~ 300 nm) having a fuzzy, hairy, interface, here referred as "cotton balls" were observed for the latter in freshly prepared samples (Figure 4d). These aggregates are likely to act as nucleation centers for the undeveloped fibril structures branching out, but do not develop into a proper hydrogel network. Derivative **KLVFF(Br)** and **WT** peptides, instead, only formed amorphous aggregates (Figure S3). Overall, obtained TEM data clearly indicated the possibility of engineering different amyloid fibril architectures by changing position, number, and nature of the halogen atoms in the peptide fragment **KLVFF**.

Due to their interesting morphologies and to ascertain whether the observed peptide nanostructures may be related to drying effects, vitrified 15 mM aqueous solutions of **KLVFF(I)** and **KLVF(Br)F(Br)** were furtherly investigated by Cryogenic-TEM (Cryo-TEM). As shown in Figure 4a$_1$, the presence of the

spherical NPs observed in the dried state was confirmed for sample **KLVFF(I)**. Imaged NPs showed smoother interface and more uniform shape when compared to NPs imaged in the dried state, indicating a possible NP agglomeration effect during the

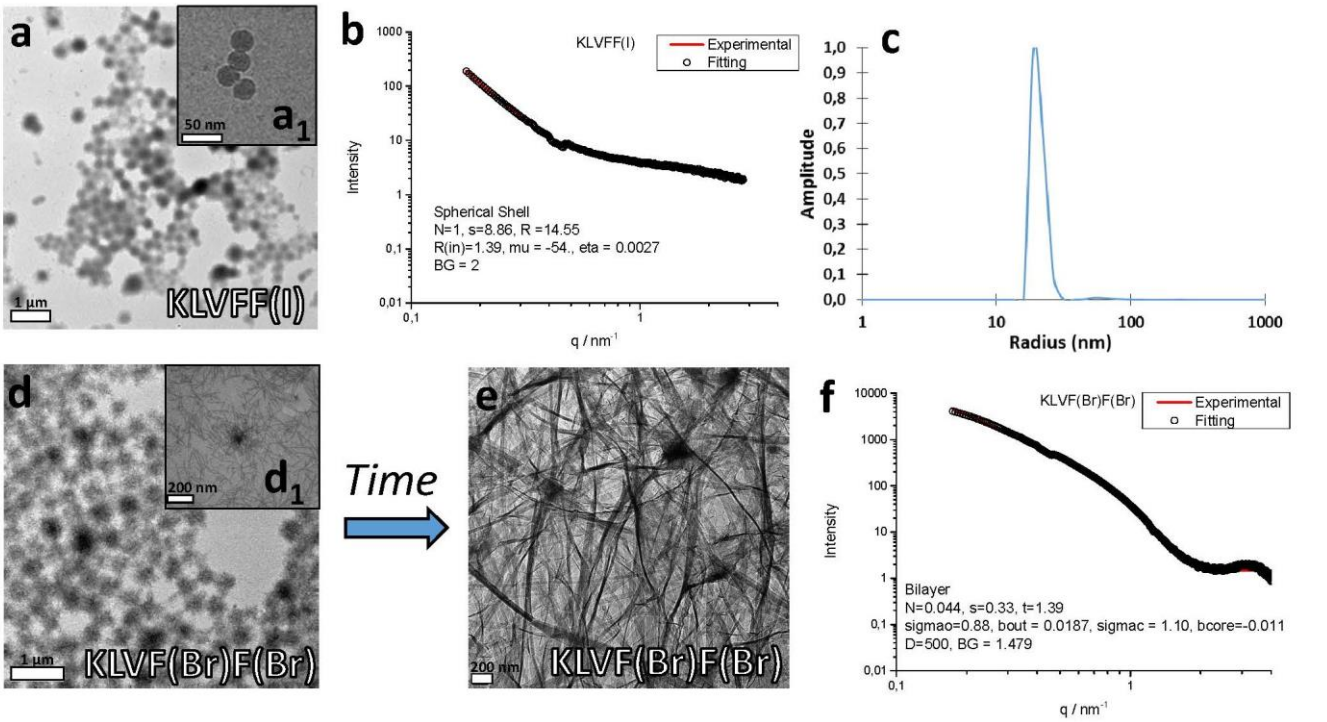

Figure 4. a) TEM image of 15 mM dried sample of **KLVFF(I)** aged for 48h; a_1) Cryo-TEM image showing the spherical nanoparticles formed by **KLVFF(I)** 15 mM; b) SAXS profile of 15 mM **KLVFF(I)** dispersion with fitting analysis according to a core-shell spherical form factor; c) Number average size distribution extracted from DLS analysis of **KLVFF(I)** 5 mM dispersion; d) TEM image of 15 mM dried sample of **KLVF(Br)F(Br)** aged for 48h; d_1) Magnification of an isolated "cotton ball" structure formed by **KLVF(Br)F(Br)** from 15 mM solution aged for a week; e) Cryo-TEM image showing an entangled fibrillar network formed by a one-month aged **KLVF(Br)F(Br)** 15 mM sample; f) SAXS profile of **KLVF(Br)F(Br)** 15 mM samples with fitting analysis according to a bilayer form factor.

state. A 5 mM water dispersion of **KLVFF(I)** was also studied by multi-angle DLS analysis giving bimodal auto-correlation functions composed of two populations characterized by 50 nm and 330 nm hydrodynamic radius, respectively (Figure S4). However, the number-averaged size distribution obtained for the same sample showed that the small population is much more abundant than the larger one, which is in agreement with microscopy results (Figure 4c).

On the other hand, cryo-TEM imaging of individual "cotton balls" formed by freshly prepared samples of **KLVF(Br)F(Br)** was not achievable as the maximum thickness detectable with this technique is about 100 nm (Figure S10).[22] However, cryo-TEM analysis on one-month aged solutions indicated the presence of an entangled network of fibers with well visible nucleation points (Figure 4e), suggesting that the "cotton balls" evolved in a more thermodynamically stable architecture such as the typical amyloid fibril network. This structural transition is also observable macroscopically, since freshly prepared 15 mM peptide solutions become more and more viscous over time until they form a gel (Figure S11).

Bulk characterization of one-month aged 15 mM peptide samples was carried out through Small Angle X-Ray Scattering (SAXS) (Figure S12). Halogenated derivatives showed a clearly different scattering behavior compared to **KLVFF**. Bragg Peaks at q = 1.5 nm^{-1} can be seen for samples **KLVF(Br)F(Br)** (Figure 4f) and **KLVF(I)F(I**) (Figure S12), indicating the presence of periodic structures with around 2 nm spacing. Scattering patterns for these two samples were fitted using a bilayer model, previously employed for tape/ribbon-like structures.[23] Obtained values indicate a bilayer thickness of 1.4 nm for the bis-brominated peptide and 0.9 nm for the bis-iodinated one. **KLVFF(I)** scattering curve was fitted by a core-shell spherical model (Figure 4b). The fitting yielded a diameter of 19.1 nm, in good agreement with size determined by cryo-TEM. Long cylindrical shell model was, instead, used to analyze **KLVFF(Br)** scattering curve (Figure S12). The fitting indicated a cylinder diameter of 5.7 nm.

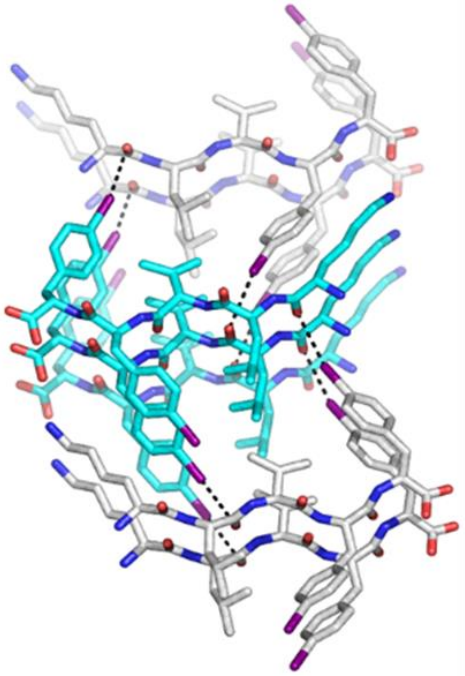

Figure 5. 'Steric zipper' motif formed by **KLVF(I)F(I)**, showing intermolecular halogen bonds among the iodine atom and the carbonyl oxygen belonging to adjacent β-sheets.

We have recently demonstrated that iodination, alongside facilitating phase determination, may be developed as a routine strategy to obtain the single-crystal X-ray structures of peptide segments otherwise difficult to crystallize. Thanks to this strategy, we have, for example, shed light on the elusive aromatic–aromatic interactions occurring in peptide segments containing phenylalanine, such as **DFNKF**[24]. With the objective of determining whether noncovalent interactions involving halogen atoms may play a role in stabilizing the nanostructures observed in the present studies, we attempted crystallization of the **KLVF(I)F(I)** derivative. Small, weakly diffracting, and poorly ordered crystals were obtained after two months upon slow evaporation of a water/hexafluoro-2-propanol 9:1 mixture (see SI). However, accurate structure solution was possible by using synchrotron radiation.

Similar to all other amyloid structures, the stacking of β-sheet pairs at the dry interface is the stable structural unit of the "cross-β-spine",[25] along which tightly interacting side chains form the self-complementary motif called "steric zipper",[26] which explains how very short peptide sequences are able to form such extended structures like amyloid fibrils (Figure S14). Interestingly, the high-resolution single-crystal structure of **KLVF(I)F(I)** shows the occurrence of intermolecular C=O···I contacts, *i.e.*, halogen bonds, between peptides belonging to adjacent β-sheets (Figure 5). The two asymmetric O···I distances are O_1···I_5 3.34(3) Å and O_2···I_4 3.43(3) Å, with C=O···I and O···I-C angles of 111(2)° and 103(2)°, and 165(1)° and 159(1)°, respectively. Importantly, the O_2···I_4 halogen bond occurs orthogonally[27] to the O_2···N_3 hydrogen bond of the β-sheet (N···O distance 2.99(3) Å; N···O···I angle 88.5(8)°). This is the first structural evidence of halogen bonding stabilizing the steric zipper of amyloidogenic peptides. The occurrence of halogen bonding causes **KLVF(I)F(I)** monomers to pair in parallel mode, while in the structure of the non-iodinated sequence **KLVFFA**, monomers pair in antiparallel mode, resulting in a different type of "steric zipper"(Figure S14). This result confirms the potential that the halogen bond has to engineer amyloidal peptide self-assembly.[14]

The high-resolution single-crystal structures of **KLVF(Br)F(Br)** and **KLVF(Cl)F(Cl)** were also obtained. The former is isostructural with **KLVF(I)F(I)** and shows a weaker halogen bonding, due to the lower polarizability of Br, while the latter shows no sign of halogen bonding as can be expected from a chlorobenzene derivative.[16]

In conclusion, herein we have reported that single-atom hydrogen-for-halogen replacement at the *p*-position of either one or both Phe benzene rings expands the structural landscape of **KLVFF**. At least four solution-stable polymorphic architectures have been obtained comprising fibrils, ribbons, nanoparticles, and "cotton balls", which are not shown by the **WT** peptide in the same experimental conditions. The position, nature, and number of the introduced halogen atoms dictate the specific formation of each determined architecture. The present hypothesis is corroborated by crystallographic determinations that fully demonstrate the potential that halogen bond has to engineer amyloidal peptide self-assembly.

ASSOCIATED CONTENT

Supporting Information

Experimental procedures, additional tables and figures. This material is available free of charge via the Internet at http://pubs.acs.org.

Supplementary material. CCDC 1454960, 1454959, and 1494096 contain the supplementary crystallographic data for peptides **KLVF(I)F(I)**, **KLVF(Br)F(Br)**, and **KLVF(Cl)F(Cl)**, respectively. These data can be obtained free of charge from the Cambridge Crystallographic Data Centre via www.ccdc.cam.ac.uk/data_request/cif.

AUTHOR INFORMATION

Corresponding Author

* pierangelo.metrangolo@polimi.it

Author Contributions

The manuscript was written through contributions of all authors. All authors have given approval to the final version of the manuscript.

Funding Sources

The European Research Council (ERC) is acknowledged for the granting the project FOLDHALO to P.M. (no. 307108). IWH thanks EPSRC (UK) for Platform grant ref. EP/L020599/1 and the ESRF for the award of beamtime (ref. MX-1769)

REFERENCES

(1) Chiti, F.; Dobson, C. M. *Annu. Rev. Biochem* **2006**, *75*, 333.
(2) Ulijn, R. V.; Smith, A. M. Chem. Soc. Rev. **2008**, *37*, 664.
(3) Cherny, I.; Gazit, E. Angew. Chemie - Int. Ed. **2008**, *47*, 4062.
(4) Branco, M. C.; Schneider, *J. P. Acta Biomater*. **2009**, *5*, 817.
(5) Aggeli, A.; Nyrkova, I. A.; Bell, M.; Harding, R.; Carrick, L.; McLeish, T. C. B.; Semenov, A. N.; Boden, *N. Proc. Natl. Acad. Sci. U.S.A.* **2001**, *98*, 11857.
(6) Hamley, I. W. Angew. Chemie - Int. Ed. **2014**, *53*, 6866.
(7) Caplan, M. R.; Schwartzfarb, E. M.; Zhang, S.; Kamm, R. D.; Lauffenburger, D. A. *Biomaterials* **2002**, *23*, 219.
(8) Elkins, M. R.; Wang, T.; Nick, M.; Jo, H.; Lemmin, T.; Prusiner, S. B.; Degrado, W. F.; Stöhr, J.; Hong, M. *J. Am. Chem. Soc*. **2016**, *138*, 9840.
(9) Berryman, J. T.; Radford, S. E.; Harris, S. A. *Biophys. J.* **2011**, *100*, 2234.
(10) Cui, H.; Cheetham, A. G.; Pashuck, E. T.; Stupp, S. I. *J. Am. Chem. Soc*. **2014**, *136*, 12461.
(11)Taraballi, F.; Campione, M.; Sassella, A.; Vescovi, A.; Paleari, A.; Hwang, W.; Gelain, F.; *Soft Matter*, **2009**, *5*, 660.

(12) Wang Y.; Qi W.; Huang R.; Yang X.; Wang M.; Su R.; He Z. *J. Am. Chem. Soc*, **2015**, *137*, 7869.
(13) Hamley, I. W.; Krysmann, M. J. *Langmuir* **2008**, *24*, 8210-8214.
(14) Bertolani, A.; Pirrie, L.; Stefan, L.; Houbenov, N.; Haataja, J. S.; Catalano, L.; Terraneo, G.; Giancane, G.; Valli, L.; Milani, R.; Ikkala, O.; Resnati, G.; Metrangolo, P. *Nat. Commun*. **2015**, *6:7574*, DOI: 10.1038/ncomms8574.
(15) Metrangolo, P.; Pilati, T.**;** Resnati, G. *CrystEngComm* **2006**, *8*, 946.
(16) Cavallo, G.; Metrangolo, P.; Milani, R.; Pilati, T.; Priimägi, A.; Resnati, G.; Terraneo, G. *Chem. Rev.*, **2016**, *116*, 2478.
(17) Gazit, E. *Nat. Chem.* **2015**, *7*, 14.
(18) Frederix, P. W. J. M.; Scott, G. G.; Abul-Haija, Y. M.; Kalafatovic, D.; Pappas, C. G.; Javid, N.; Hunt, N. T.; Ulijn, R. V; Tuttle, T. *Nat. Chem.* **2015**, *7*, 30.
(19) Steed, J.W. *Chem.Commun*., **2011**, *47*, 1379.
(20) Krysmann, M. J.; Castelletto, V.; Kelarakis, A.; Hamley, I. W.; Hule, R. A; Pochan, D. J. Biochemistry **2008**, *47*, 4597.
(21) Abbas, M.; Zou, Q.; Li, S.; Yan, X.; Adv. Mater. **2017**, *29*, DOI: 10.1002/adma.201605021.
(22) Glaeser, R. M. Nat Methods **2016**, *13*, 28.
(23) Hamley, I. W; Dehsorkhi, A.; Castelletto, V. *Chem. Commun.* **2013**, *49*, 1850.
(24) Bertolani, A., Pizzi, A., Pirrie, L., Gazzera, L., Morra, G., Meli, M., Colombo, G., Genoni, A., Cavallo, G., Terraneo, G., Metrangolo, P. *Chem. Eur. J.* **2017**, *23*, 2051.
(25) Nelson, R.; Sawaya, M. R.; Balbirnie, M.; Madsen, A. Ø.; Riekel, C.; Grothe, R.; Eisenberg, D. *Nat. Cell Biol*. 2005, *435*, 773**.**
(26) Stroud, J. C. *Acta Crystallogr. Sect. D Biol. Crystallogr*. **2013**, *69*, 540.
(27) Vasylyeva, V.; Nayak, S. K; Terraneo, G.; Cavallo, G.; Metrangolo, P.; Resnati, G. *CrystEngComm*,**2014**, *16*, 8102.